Aero2015P201

The 14th International Conference of Iranian Aerospace Society
Communication and Space Technology, Iranian Research Organization for Science and Technology, Tehran, 3th to 5th of March, 2015.

The 14th International Conference of Iranian Aerospace Society

Uniform Flight Path Planning for surveillance and obstacle avoidance based on stable limit cycle concept

A. Hakimi[1], T. Binazadeh[2], M.H. Shafiei[3],
Department of Electrical and Electronic Engineering
Shiraz University of Technology, Shiraz, Iran

Abstract
This paper proposes a method to generate a uniform flight path for surveillance of a region, using the limit cycle concept. The proposed method is based on the limit cycle characteristic of second order nonlinear systems for real-time flight path planning for UAVs. The generated flight path covers whole area of a circle with arbitrary radius and density of the trajectories. UAVs by tracking such trajectories are able to get the precise aerial photos or movies (or another task which needs such a trajectory). The proposed real-time flight path is divided to three main phases; in the first phase, the UAV takes off from the launch station and moves to the near of the center of the considered circular sightly area for getting the aerial photos or movies. This phase is also done based on the limit cycle navigation method to generate the safe trajectory against the obstacles (obstacle avoidance using limit cycle navigation). In the second phase, the flying object tracks a uniform helicoidal trajectory to reach the circular limit cycle, to scan a circular sightly area, completely. In the last phase, when the scanning of the sightly area has been accomplished, the UAV comes back to the launch station on the trajectory that produced by a similar procedure of the first phase. Finally, some simulations are carried out to show the flight path generated by this idea.

Keywords: *circular limit cycle- path planning- obstacle avoidance- UAV*

Introduction

Limit cycles (or non-trivial periodic orbit) occur in some of nonlinear systems that lead to stable periodic solutions. These solutions oscillate in the constant frequency and amplitude for all initial conditions in the attraction domain. In some unforced systems, this property exists on their own, while for forced systems, it may needs to design a control input to achieve the desired limit cycle [1].

This property has been employed for various applications. For example, generation of the required limit cycle motion for a robot was studied in [2]. A CLF control strategy based on limit cycles for planar space robot was proposed in [3]. Also, application of limit-cycle for obstacle avoidance in robots and UAVs was studied in [4] and [5, 7].

This paper, considers the last application which also called limit cycle navigation. This idea was firstly proposed for mobile robots that move in *x-y* coordinate [4]. Then, this strategy was generalized to UAVs in 3D for flight path planning for obstacle avoidance [7]. In this paper, in addition to obstacle avoidance, the asymptotically stable circular limit cycles are used to generate a uniform flight path for surveillance of a region which may be done for different purposes like area mapping, observations, fire and damage assessment, and so on. All of these applications need to scan the entire interior of the sightly area. Some trajectories have been proposed in literatures for this purpose. For example in [8], four different trajectories are considered. However, the proposed trajectories are not uniform and may not be able to cover all of the considered area. Also, it is possible that the UAV can't track these non-uniform path flights. Whereas in this paper, a circular limit cycle with the desirable radius is generated and a helicoidal flight path trajectory is constructed which uniformly converges to the circular limit cycle.

The suggested flight path is consisting of three phases. In the first phase, the UAV takes off from the launch station and moves to the near of the center of the considered sightly area. In this phase, for obstacle avoidance, a safe trajectory is generated using limit cycle navigation. In the second phase, the flying object tracks a uniform helicoidal trajectory with desirable density to reach the stable circular limit cycle and in the last phase; the UAV comes back to the launch station by a similar procedure of the first phase for obstacle avoidance. Finally, some simulations are performed to show the flight path generated by this idea.

The UAV Model

There are different classifications for UAVs (based on their application, structure and so on). In one of these classifications, the UAVs divided in two categories: fixed-wing aircrafts and rotary-wing aircrafts. Rotorcrafts are a kind of rotary-wing aircrafts, which have special characteristics compare with fixed-wing aircrafts. For example, rotorcrafts are able to fly and hover in low altitude. Furthermore, vertically takeoff and landing in the limited space, is another characteristic of this category of s UAVs. Quad rotor is one configuration of rotorcrafts that includes four rotors, arranged in '+' shape (Fig.1) and can be directed to any position by changing the fixed-pitch rotor's speed. By balancing the forces produced by each rotor, it can flies precisely and achieve stable hovering [6]. As shown in Fig.1, the front and rear rotors, rotate counter clockwise and lateral rotors, rotate clockwise. Increasing the speed of all rotors simultaneously, leads to increasing the altitude of the quad rotor. To move forward, the speed of front rotor

1. Master student, Tel: 09138594828, email address :a.hakimi@sutech.ac.ir (corresponding author)
2. Assistant professor
3. Assistant professor

decreases and the speed of rear rotor increases, whereas the speeds of the lateral rotors are the same and constant. Also to move right, the speed of the right rotor decreases and the speed of the left rotor increases, whereas the speeds of the front and rear rotors are the same and constant.

Many studies have been done on the control of quad rotor [9-11]. To control the Euler angles, the front and rear rotors are used. Also, the lateral rotors can control the roll angle. For clockwise rotation (in the yaw direction), speeds of the lateral rotors increase and speeds of front and rear rotors decrease in such a way that the total thrust of rotors is constant [12].

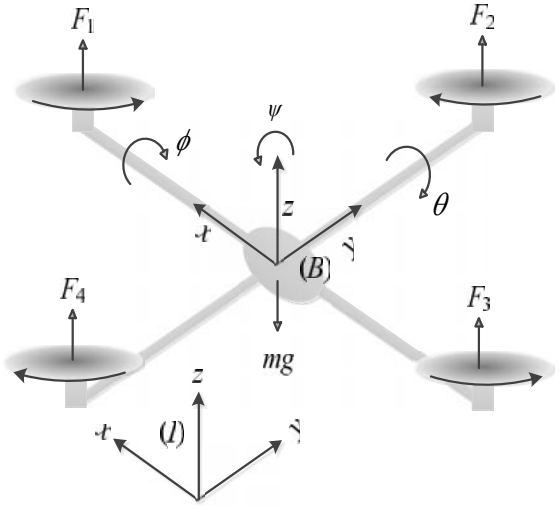

Fig.1 The quad rotor's structure and the corresponding coordinate systems

To describe the dynamic of a quad rotor, the inertial reference frame (I) and the body-fixed frame (B) should be considered. Based on the Euler angles, the rotational matrix between these frames is as follows:

$$R_{IB} = \begin{bmatrix} C_\theta C_\psi & C_\psi S_\theta S_\phi - C_\phi S_\psi & C_\phi S_\theta C_\psi + S_\phi S_\psi \\ C_\theta S_\psi & S_\theta S_\phi S_\psi - C_\phi C_\psi & C_\phi S_\theta S_\psi - C_\psi S_\phi \\ -S_\theta & C_\theta S_\phi & C_\theta C_\phi \end{bmatrix} \quad (1)$$

where C and S are abbreviates of cosine and sine functions. Also θ, Φ and ψ are pitch, roll and yaw angles (Euler angles), respectively.

Now, the transformation of the vectors position, velocity, moment, force and so on between the inertial reference frame and the body-fixed frame can be calculated based on the rotational matrix R_{IB}. Also, the rotational dynamics of the system can be derived using the Newton's law. Consequently, the dynamic equations of the quad rotor are as follow [7]:

$$\begin{aligned} \ddot{x} &= \frac{\cos\phi\cos\psi\sin\theta + \sin\phi\sin\psi}{m}\sum_{i=1}^{4} F_i \\ \ddot{y} &= \frac{\cos\phi\sin\theta\sin\psi - \cos\psi\sin\phi}{m}\sum_{i=1}^{4} F_i \\ \ddot{z} &= \frac{\cos\phi\cos\theta\sum_{i=1}^{4} F_i}{m} - g \\ \ddot{\phi} &= \frac{l}{I_x}(F_4 - F_2) \\ \ddot{\theta} &= \frac{l}{I_y}(F_3 - F_1) \\ \ddot{\psi} &= \frac{1}{I_z}(F_1 + F_3 - F_2 - F_4) \end{aligned} \quad (2)$$

where m is the quad rotor's mass, g is the gravity acceleration and l is the distance from the center of mass of the quad rotor and the center of each rotor. Also I_x, I_y and I_z are moments of inertia of the quad rotor and $F_i, i = 1,2,3,4$ are the produced forces by each of the four rotors.

The Circular Limit Cycle

In this section, the circular limit cycle characteristic of a second order nonlinear system is introduced and the asymptotical stability of this limit cycle is investigated based on the Lyapunov theorem [13].

Consider the following nonlinear system:

$$\begin{aligned} \dot{x}_1(t) &= -x_2(t) + \alpha x_1(t)(\lambda^2 - x_1(t)^2 - x_2(t)^2) \\ \dot{x}_2(t) &= x_1(t) + \alpha x_2(t)(\lambda^2 - x_1(t)^2 - x_2(t)^2) \end{aligned} \quad (3)$$

where $x = [x_1 \ x_2]^T \in \sqcup^2$ is the state vector. Also α and λ are positive parameters and will be discussed later. Now, consider the Lyapunov function as;

$$V(x(t)) = x_1(t)^2 + x_2(t)^2 \quad (4)$$

Calculating $\dot{V}(x) = (\partial V / \partial x)\dot{x}$, along the trajectories of system (3), leads to:

$$\begin{aligned} \dot{V}(x(t)) &= 2x_1\dot{x}_1 + 2x_2x_2 \\ &= 2x_1x_2 + 2\alpha x_1^2(\lambda^2 - x_1^2 - x_2^2) \\ &\quad -2x_1x_2 + 2\alpha x_2^2(\lambda^2 - x_1^2 - x_2^2) \\ &= 2\alpha V(x(t))(\lambda^2 - V(x(t))). \end{aligned} \quad (5)$$

Define the following invariant set [13]:

$$\begin{aligned} \Gamma: &\{x \in \sqcup^2 \ s.t. \ \dot{V}(x) = 0\} \\ &= \{x \in \sqcup^2 : V(x) = 0, V(x) = \lambda^2\} \end{aligned} \quad (6)$$

In this set, $\dot{V}(x(t)) = 0$ results in $x_1(t) = x_2(t) = 0$, which is the equilibrium point of the system (3). Also, $V(x(t)) = \lambda^2$ results in $x_1(t)^2 + x_2(t)^2 = \lambda^2$, which shows that the circle with radius λ is a limit cycle of the system (3).

In what follows, the asymptotical stability of this circular limit cycle is investigated (based on the Lyapunov theorem) in two cases:

Case 1: Consider the initial condition $x(t_0) = x_0 \neq 0$ in the interior of the circle with radius λ. Thus $V(x(t_0)) = \alpha$ where $0 < \alpha < \lambda^2$. Therefore, according to (5), $\dot{V}(x)$ is positive and $V(x)$ increases until it reaches to $V(x(t)) = \lambda^2$ and $\dot{V}(x)$ converges to zero (Dashed lines in Fig.2 show trajectories in this case for some initial conditions assuming α=λ=1).

Case 2: Consider the initial condition $x(t_0) = x_0 \neq 0$ in the exterior of the circle with radius λ. Thus $V(x(t_0)) = \beta$, where $\beta > \lambda^2$ and therefore, according to (5), $\dot{V}(x(t))$ is negative and $V(x(t))$ decreases until it converges to $V(x(t)) = \lambda^2$ and $\dot{V}(x)$ converges to zero (Solid lines in Fig.2 show trajectories in this case for some initial conditions assuming α=λ=1).

As seen, parameter λ is the radius of the circular limit cycles generated by (3). Also, trajectories converge to the circular limit cycles in the counter clockwise direction.

Now consider the following nonlinear system:

$$\begin{aligned} \dot{x}_1(t) &= x_2(t) + \alpha x_1(t)(\lambda^2 - x_1(t)^2 - x_2(t)^2) \\ \dot{x}_2(t) &= -x_1(t) + \alpha x_2(t)(\lambda^2 - x_1(t)^2 - x_2(t)^2) \end{aligned} \qquad (7)$$

where parameters are the same as the system (3). Repeating the similar corollaries which was carried out for the nonlinear system (3), it is found out that the system (7) also has a circular limit cycle with radius λ but in the clockwise direction. Fig.3 shows trajectories of (7) for some initial conditions (assuming α=λ=1).

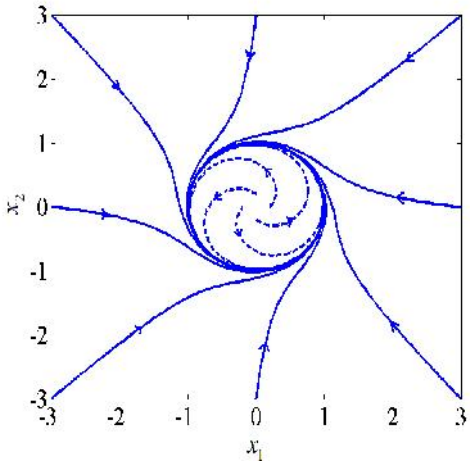

Fig.2 Counter clockwise convergence of trajectories of system (3) to unit circle

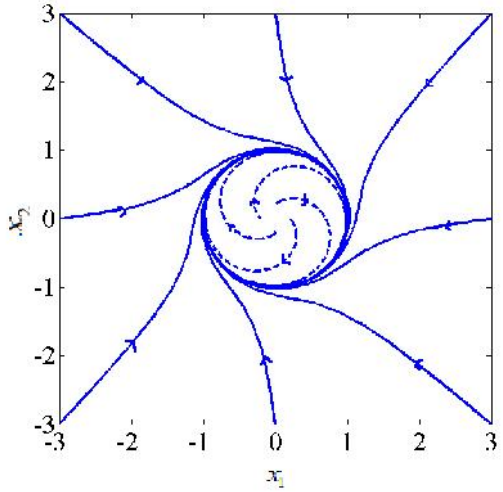

Fig.3 Clockwise convergence of trajectories of system (7) to unit circle

Limit Cycle Navigation Scheme

This section introduces two main different practical aspects of using limit cycle for path planning: obstacle avoidance and uniform scanning of an area.

The UAV uses these two aspects of limit cycle to generate the real-time flight path for its mission.

A. Obstacle avoidance using the circular limit cycle

Consider the quad rotor situated in the rightmost of Fig.4. In moving towards the goal, it should avoid obstacles (for example tall building, trees or mountains).

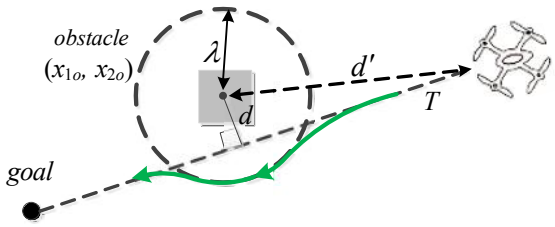

Fig.4 Obstacle avoidance using circular limit cycle

The steps to pass these obstacles without collision are as follow [4]:

I: Consider a straight line T from the quad rotor to the goal in x_1-x_2 plane as:

$$ax_1 + bx_2 + c = 0 \qquad (8)$$

II: Move to goal on the line T as long as there is not any obstacle. When approaching to an obstacle (it means $d' \sqcup \rho\lambda, 1 < \rho \leq 2$, where d' is the distance from quad rotor to center of obstacle and λ is the obstacle radius plus safety margin for collision avoidance), calculate the distance d from the center of the obstacle (x_{1o}, x_{2o}) to the line T by the following equation:

$$d = \frac{ax_{1o} + bx_{2o} + c}{\sqrt{a^2 + b^2}} \tag{9}$$

III: Calculate the dynamics of the desired trajectory by substituting d and λ and also $\alpha = 2$ in the following equation:

$$\begin{aligned} \dot{x}_1(t) &= \frac{d}{|d|} x_2(t) + \alpha x_1(t)(\lambda^2 - x_1(t)^2 - x_2(t)^2) \\ \dot{x}_2(t) &= -\frac{d}{|d|} x_1(t) + \alpha x_2(t)(\lambda^2 - x_1(t)^2 - x_2(t)^2) \end{aligned} \tag{10}$$

Note that for $d > 0$, the quad rotor avoids obstacle clockwise whereas for $d < 0$, the quad rotor avoids obstacle counter clockwise.

IV: Calculate the line $T'(a'x_1 + b'x_2 + c' = 0)$ from quad rotor to goal in each time of motion on the limit cycle. Exit from circular limit cycle trajectory when $a' = a, b' = b, c' = c$ .Then moves on line T until to reach the goal.

B. Scanning an area using the circular limit cycle

The aim of this subsection is to make a uniform trajectory that scans whole of a circular area with radius λ (dashed circle in Fig.5) by the circular limit cycle trajectory.

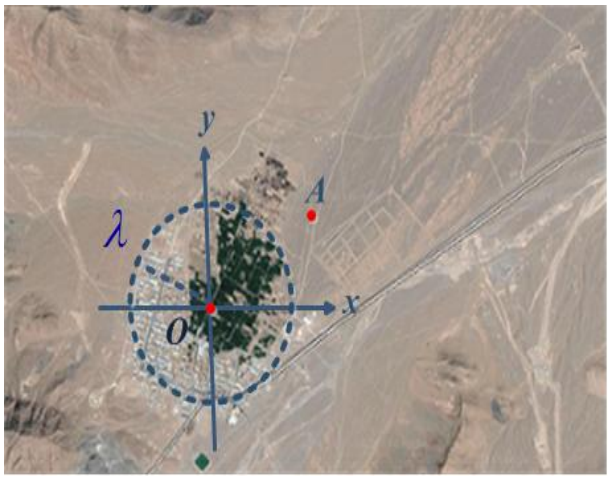

Fig.5 The sightly area for scanning by the circular limit cycle

For this purpose, consider the nonlinear system (3) again:

$$\begin{aligned} \dot{x}_1(t) &= -x_2(t) + \alpha x_1(t)(\lambda^2 - x_1(t)^2 - x_2(t)^2) \\ \dot{x}_2(t) &= x_1(t) + \alpha x_2(t)(\lambda^2 - x_1(t)^2 - x_2(t)^2) \end{aligned} \tag{11}$$

Assume the initial position in the interior of the circle near to the origin O. Fig.6 shows trajectories of (11) for λ=1 and some different values of α.

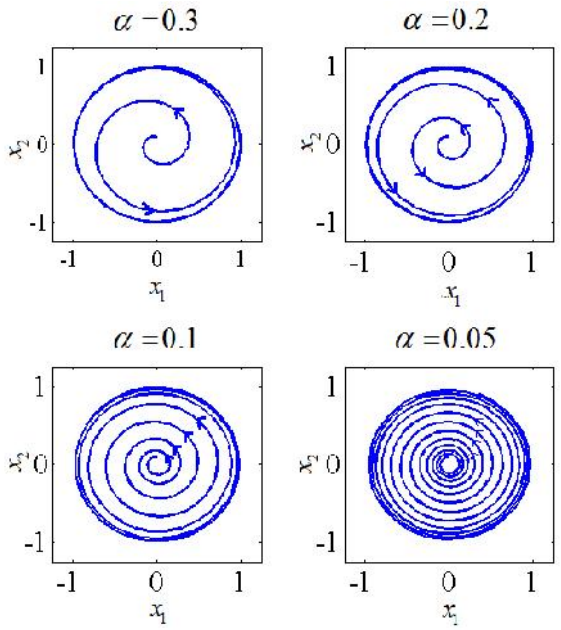

Fig.6 Trajectories of (11) for some different values of α

As shown, the dynamical equation (11) produces a uniform helicoidal trajectory which can scan whole of the circular area with the radius λ. Also, the scalar parameter α effects on the density of the trajectories, such that less value for α leads to more dense trajectories.

The Proposed Real-Time Flight Path

In this section, the proposed real-time flight path using the circular limit cycle is discussed in details. Actually, this idea is the combination of the trajectories, generated in each subsections of the previous section.

Consider Fig.5 again. The launch station is situated at the point A. The aim is getting aerial photos or movie from the hatched area. For this purpose, a circle with radius λ is considered on the sightly area in the height h. The quad rotor takes off from point A and moves to the defined height (h) near to point O. Next, it flies in a helicoidal trajectory with the constant height referring to an asymptotically stable circular limit cycle until reaches to the defined circle with radius λ. Then, it comes back and lands to the point A. Also, in the takeoff and landing phases, there are obstacles in fight path.

The flight trajectory is divided into three phases:
Phase 1: Move from the point A (with position (x_0, y_0, 0)) to the point B (with position (x_1, y_1, h) where $r_1 = (x_1^2 + y_1^2)^{1/2} > 0$ is small enough) on the trajectory C_1, as shown in Fig.7 (a). The trajectory C_1 in the z-r coordinates is as follows:

$$C_1 : \; z(r) = a_3 r^3 + a_2 r^2 + a_1 r + a_0 \tag{12}$$

where $r = (x^2 + y^2)^{1/2}$ and also $z(r)$ satisfies the following constraints:

$$z(r_0) = 0,\; z(r_1) = h,\; \dot{z}(r_0) = 0,\; \dot{z}(r_1) = 0 \tag{13}$$

where $r_0 = (x_0^2 + y_0^2)^{1/2}$. Fig.7(b) shows the top view of this situation. It is assumed that in the quad rotor's way to the point B, there are obstacles O_1 and O_2. The quad rotor passes O_1 in the counter clockwise direction and next, passes O_2 in the clockwise direction based on the first subsection of previous section but in 3-dimentional. Also, in Fig.7 (b), C_1' is the projection of C_1 in x-y plane.

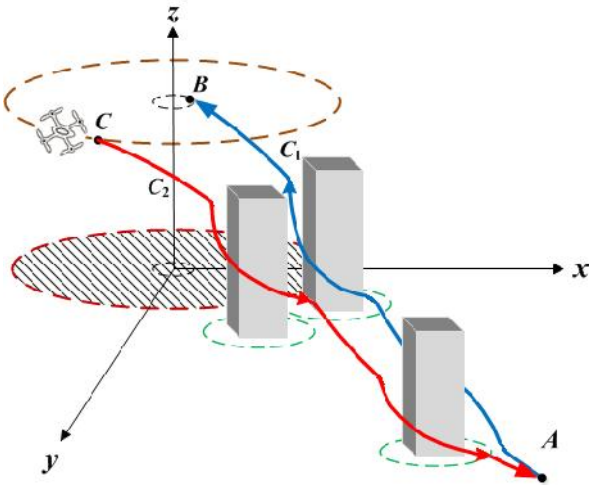

(a)

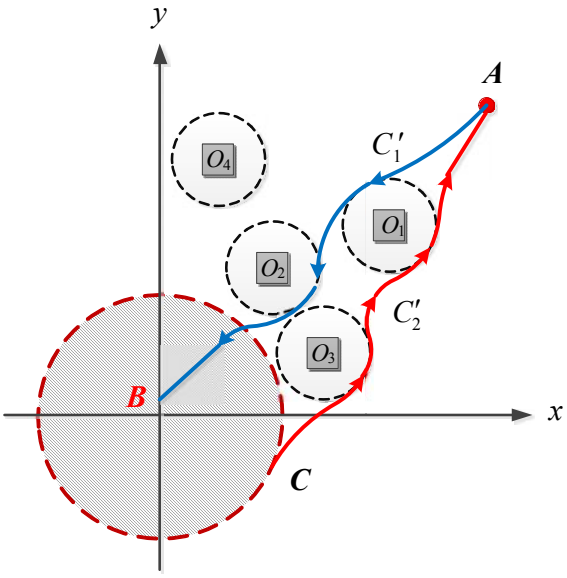

(b)

Fig.7 First and third part of trajectory,
(a) 3-D view; (b) top view

Phase 2: The aim of this phase is making the uniform trajectory that scans whole of the hatched area in Fig.7 (a). For this purpose, the quad rotor moves on the trajectory, generated by system (11) based on the second subsection of the previous section. Parameter α is specified based on the required accuracy. Also, the point B is the start point (initial condition) for system (11).

This part terminates when scanning of the area with radius $r=\lambda$ is carried out, completely. In Fig.7(a), the point C (with position (x_2, y_2, h)) is considered as the end point of this phase.

Phase 3: Come back from the point C to the point A on the trajectory C_2, as shown in Fig.7 (a), where the trajectory C_2 in the z-r coordinates is as follows

$$C_2 : z'(r) = a_3' r^3 + a_2' r^2 + a_1' r + a_0' \qquad (14)$$

where $z'(r)$ satisfies the following constraints:

$$z'(r_0) = 0,\ z'(r_2) = h,\ \dot{z}'(r_0) = 0,\ \dot{z}'(r_2) = 0 \qquad (15)$$

Also, $r_0 = (x_0^2 + y_0^2)^{1/2}$ and $r_2 = (x_2^2 + y_2^2)^{1/2}$. Similar to first phase, in the quad rotor's way back to point A, there are obstacles O_1 and O_3. The quad rotor passes first O_3 and then O_1 in the counter clockwise direction. Also in Fig.7 (b), C_2' is the projection of C_2 in x-y plane.

Simulation

Consider that we need to uniformly scan the circular area with radius λ=1300m. The point A is situated at the position (4000, 4000, 0). In the flying object's way, there are obstacle O_1 in the position (1620 ,1580 ,0) with 80m tall and also obstacle O_2 in position (2390 ,1720 ,0) with 110m tall. Also the desired height for scanning area is considered as h=150 m. taking α = 0.2 fulfills required accuracy in photos. Fig.8, presents the trajectory, produced by the suggested flight path planning using limit cycle navigation scheme.

As shown in Fig.8, the quad rotor takes off from point A. In its way to point B, it faces an obstacle O_1. The quad rotor avoids an obstacle in the clockwise direction. Then continues to its way until reaches to point B with the position (- 40, 30, 150). Then it begins to scan sightly area in the constant height, h. After that, the quad rotor scans the area, completely, it exits from the circular limit cycle trajectory in the point C with the position (1104, - 332, 150). Next moves on come back trajectory. In its way, there is an obstacle O_2. The quad rotor avoids this obstacle in the clockwise direction too and reaches to initial position.

Conclusion

The main aim of this paper was generating the uniform flight path for a quad rotor to scan the whole of a circular area. For this purpose, the idea of quad rotor flight path planning based on the limit cycle concept was introduced and implemented for generation of helicoidal flight trajectories that covers all of the sightly area. First, the quad rotor takes off and moves to center of sightly area in the defined height, considering obstacle avoidance approach as discussed. Then it starts to move on helicoidal limit cycle trajectory, to do its defined mission, until reaches to desired radius, based on proposed limit cycle navigation scheme. Finally, comes back and lands to initial position in a similar procedure that

follows in take off phase. Some simulations carried out to generate the flight path based on the proposed idea.

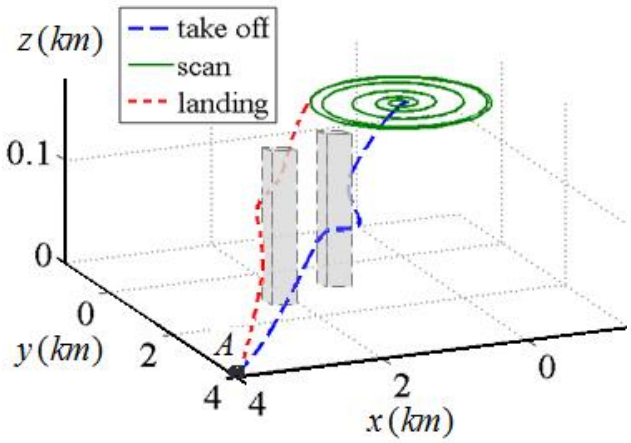

Fig.8 The flight path of the quad rotor

References

[1] W. M. Haddad and V. Chellaboina, *Nonlinear dynamical systems and control: a Lyapunov-based approach*. Princeton University Press, 2008.

[2] W. Schiehlen and N. Guse, "Control of limit cycle oscillations," in *IUTAM Symposium on Chaotic Dynamics and Control of Systems and Processes in Mechanics*, 2005, pp. 429–439.

[3] T. Kai, "Limit-cycle-like control for planar space robot models with initial angular momenta," *Acta Astronaut.*, vol. 74, pp. 20–28, May 2012.

[4] D.-H. Kim and J.-H. Kim, "Limit-cycle navigation method for soccer robot," in *International Conference on Artificial Intelligence, Las Vegas*, 2001.

[5] F. Akbar and Y. M. Mustafah, "Improved 3D limit-cycle navigation method for path planning quad rotor," *IOP Conf. Ser. Mater. Sci. Eng.*, vol. 53, p. 012084, Dec. 2013.

[6] P. C. Garcia, R. Lozano, and A. E. Dzul, *Modelling and control of mini-flying machines*. Springer, 2006.

[7] B. C. Min, E. J. Lee, S. H. Kang, and D. H. Kim, "Limit-cycle navigation method for a quad-rotor type UAV," in *Industrial Electronics, 2009. ISIE 2009. IEEE International Symposium on*, 2009, pp. 1352–1357.

[8] M. Barbier and E. Chanthery, "Autonomous mission management for unmanned aerial vehicles," *Aerosp. Sci. Technol.*, vol. 8, no. 4, pp. 359–368, Jun. 2004.

[9] P. Melin and O. Castillo, "Adaptive intelligent control of aircraft systems with a hybrid approach combining neural networks, fuzzy logic and fractal theory," *Appl. Soft Comput.*, vol. 3, no. 4, pp. 353–362, Dec. 2003.

[10] Y. Morel and A. Leonessa, "Direct adaptive tracking control of quadrotor aerial vehicles," in *ASME 2006 International Mechanical Engineering Congress and Exposition*, 2006, pp. 155–161.

[11] K. Peng, G. Cai, B. M. Chen, M. Dong, K. Y. Lum, and T. H. Lee, "Design and implementation of an autonomous flight control law for a UAV helicopter," *Automatica*, vol. 45, no. 10, pp. 2333–2338, Oct. 2009.

[12] K. W. Weng and M. S. B. Abidin, "Design and control of a quad-rotor flying robot for aerial surveillance," in *Research and Development, 2006. SCOReD 2006. 4th Student Conference on*, 2006, pp. 173–177.

[13] H. K. Khalil and J. W. Grizzle, *Nonlinear systems*, vol. 3. Prentice hall Upper Saddle River, 2002.